# Realization of asymmetric optical filters using asynchronous coupled-microring resonators

**Ashok M. Prabhu and Vien Van**

*Department of Electrical & Computer Engineering, University of Alberta, Edmonton, Alberta, Canada T6G 2V4.*
*Email: ashok.prabhu@ualberta.ca*

**Abstract:** General filter architectures based on asynchronously-tuned, coupled-microring resonators are proposed for realizing optical filters with asymmetric spectral responses. Asymmetric filters enable more complex spectral shapes to be realized which can better meet the demands of more advanced applications than symmetric filters. By adjusting individual transmission zeros of the filter transfer function, the transition bands on the low and high-frequency sides of the passband can be separately optimized to achieve an optimum filter response. A method for synthesizing asymmetric spectral responses based on the energy coupling matrix will also be presented along with numerical examples of high-order asymmetric optical filters. These devices represent new microring-based architectures that can be explored for advanced applications in optical spectral shaping and dispersion engineering.



**OCIS codes:** (130.3120) Integrated optics devices; (250.5300) Photonic integrated circuits;

## References

1. J. V. Hryniewicz, P. P. Absil, B. E. Little, R. A. Wilson and P.-T. Ho, "Higher order filter response in coupled microring resonators," IEEE Photon. Technol. Lett. **12**, 320–322 (2000).
2. B. E. Little, S. T. Chu, P. P. Absil, J. V. Hryniewicz, F. G. Johnson, F.Seiferth, D. Gill, V. Van, O. King and M. Trakalo, "Very high order microring resonator filters for WDM applications," IEEE Photon. Technol. Lett. **16**, 2263–2265 (2004).
3. T. Barwicz, M. Popovic, P. Rakich, M. Watts, H. Haus, E. Ippen and H. Smith, "Microring-resonator-based add-drop filters in SiN: fabrication and analysis," Opt. Express **12**, 1437–1442 (2004).
4. B. E. Little, S. T. Chu, J. V. Hryniewicz and P. P. Absil, "Filter synthesis for periodically coupled microring resonators," Opt. Lett. **25**, 344–346 (2000).
5. R. Grover, V. Van, T. A. Ibrahim, P. P. Absil, L. C. Calhoun, F. G. Johnson, J. V. Hryniewicz and P.-T. Ho, "Parallel-cascaded semiconductor microring resonators for high-order and wide-FSR filters," J. Lightw. Technol. **20**, 900–905 (2002).
6. K. Jinguji, "Synthesis of coherent two-port optical delay-line circuit with ring waveguides," J. Lightwave Technol. **14**, 1882–1898 (1996).
7. C. K. Madsen, "Efficient architectures for exactly realizing optical filters with optimum bandpass design," IEEE Photon. Technol. Lett. **10**, 1136–1138 (1998).
8. V. Van, "Synthesis of elliptic optical filters using mutually-coupled microring resonators," J. Lightw. Technol. **25**, 584–590 (2007).
9. M. A. Prabhu and V. Van, "General two-dimensional coupled-cavity microring filter architectures," in *IEEE Conference on Lasers and Electro-Optics*, 2007, paper JTuA31.
10. M. A. Popovic, "Sharply-defined optical filters and dispersionless delay lines based on loop-coupled resonators and 'negative' coupling," in *IEEE Conference on Lasers and Electro-Optics*, 2007, paper CThP6.
11. H. C. Bell, "Canonical asymmetric coupled-resonator filters," IEEE Trans. Microwave Theory Technol. **30**, 1335–1340 (1982).
12. A. E. Williams, J. I. Upshur and M. M. Rahman, "Asymmetric response bandpass filter having resonators with minimum couplings," U.S. patent 6337610 (2002).
13. B. E. Little, S. T. Chu, H. A. Haus, J. Foresi and J.-P. Laine, "Microring resonator channel dropping filters," J. Lightw. Technol. **15**, 998–1005 (1997).
14. A. E. Atia and A. E. Williams, "Narrow-bandpass waveguide filters," IEEE Trans. Microwave Theory Technol. **20**, 258–265 (1972).

#82796 - $15.00 USD Received 7 May 2007; revised 9 Jul 2007; accepted 16 Jul 2007; published 19 Jul 2007

15. A. E. Atia, A. E. Williams and R. W. Newcomb, "Narrow-band multiple-coupled cavity synthesis," IEEE Trans. Circuits Syst. **21**, 649–655 (1974).
16. M. H. Chen, "Singly terminated pseudo-elliptic function filter," COMSAT Technol. Rev. **7**, 527–541 (1977).
17. R. J. Cameron, "General coupling matrix synthesis methods for Chebyshev filtering functions," IEEE Trans. Microwave Theory Technol. **47**, 433–442 (1999).
18. R. J. Cameron, "Advanced coupling matrix synthesis techniques for microwave filters," IEEE Trans. Microwave Theory Technol. **51**, 1–10 (2003).

## 1. Introduction

Microring resonators have been demonstrated to have many potential applications in optical spectral shaping, the most common application being high-order optical add/drop filters for WDM systems [1–3]. Several different microring coupling topologies for realizing box-like filter transfer functions have been proposed, such as serially-coupled microrings [2], parallel-cascaded microrings [4,5], and microring-loaded Mach-Zehnder structures [6,7]. Among these, the serial coupling topology is the most widely used because the device structure is simple and filter synthesis is relatively straightforward. The drawback of serially-coupled microring filters, however, is that they can only have all-pole transfer functions, such as those of the Butterworth and Chebyshev types. For more advanced applications requiring very high levels of frequency discrimination, isolation and out-of-band rejection, it may be necessary to include transmission zeros in the transfer function to achieve the desired spectral performance. These filters are generally of the inverse Chebyshev or elliptic type. It has been shown that Mach-Zehnder interferometers (MZI) loaded with all-pass microring resonators can be used to realize such filter responses [6,7]. Recently an alternate elliptic filter architecture was proposed which consists of a two dimensional array of mutually-coupled, synchronously-tuned microring resonators [8–10]. The coupled-cavity filter architecture does not require the use of Mach-Zehnder structures and is therefore more compact than microring-loaded MZI filters.

All the optical filters considered to date are characterized by symmetrical spectral responses, whose poles and zeros appear in complex conjugate pairs and are symmetrically located about the center frequency. In some applications, however, it may be desirable for the filter to have a skewed spectral response with one side having a much sharper frequency transition than the other. These asymmetric filters have been realized at the microwave frequencies [11,12] and are characterized by unpaired complex zeros that are unevenly distributed about the center frequency. By moving some or all of the zeros to one side of the passband, an asymmetric spectral response can be obtained which exhibits much more pronounced frequency transition and out-of-band rejection level than its symmetric counterpart. Moreover, the ability to arbitrarily position the poles and zeros of a filter enables complex amplitude and phase responses to be realized, which can have important applications in optical filtering, spectral shaping and dispersion engineering. In this paper we propose and demonstrate the use of asynchronously-tuned, coupled-microring resonators for realizing high-order asymmetric spectral responses. As it will be shown, asynchronicity offers more design flexibility in the synthesis of both symmetric and asymmetric spectral responses than synchronously-tuned devices. Thus given a transfer function, alternate filter designs can be obtained from which an optimum architecture may be selected which best meets the specific layout, fabrication, or other practical constraints. The proposed asymmetric filter architectures based on coupled-microring resonators potentially provide new avenues for exploring advanced applications of micro and nanoresonators in optical spectral shaping and dispersion engineering.

The outline of the paper is as follows. We begin in Section 2 with a description of the general coupling topology of asynchronously-tuned microring resonators. A general filter synthesis technique based on the energy coupling matrix will also be presented, followed by

#82796 - $15.00 USD Received 7 May 2007; revised 9 Jul 2007; accepted 16 Jul 2007; published 19 Jul 2007

numerical examples of asymmetric filter designs in Section 3. Concluding remarks are given in Section 4.

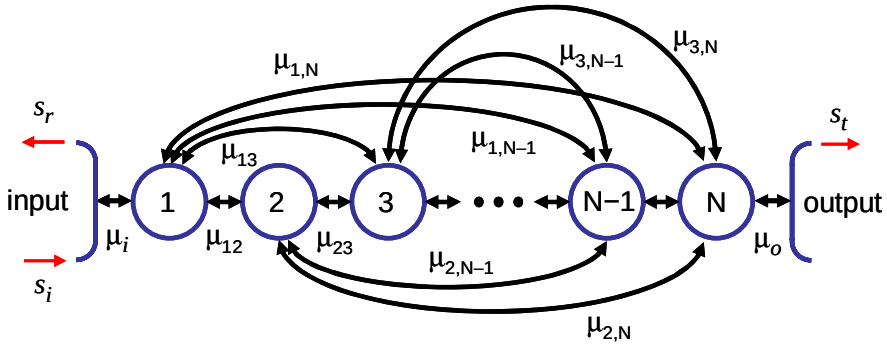


Fig. 1. Schematic of the most general coupling topology of $N$ asynchronously-tuned microring resonators in which every microring $i$ is assumed to be coupled to every other microring $j$ via energy coupling coefficient $\mu_{i,j}$.

## 2. General asynchronously-tuned coupled-microring filter topology

Figure 1 shows a schematic of the most general coupling topology of $N$ microring resonators in which every resonator is assumed to be coupled to every other resonator. In the narrow-band approximation where the filter bandwidth is much smaller than the free spectral range (FSR) of the microrings, the behavior of the system of coupled cavities in Fig. 1 may be conveniently described in terms of energy coupling in the time domain [13]. Adopting the energy coupling formalism, we denote $\mu_{i,j}$ as the energy coupling coefficient between microrings $i$ and $j$. The input and output couplings $\mu_i$ and $\mu_o$ represent the energy coupling between microring 1 and the input bus waveguide and between microring $N$ and the output bus waveguide, respectively. The input, transmitted and reflected signals are denoted by $s_i$, $s_r$ and $s_t$, respectively. The transmitted signal gives rise to the drop-port response of the filter while the reflected signal yields the through-port response. For generality we also assume that all the resonators are detuned from each other, with the amount of detuning of microring $i$ measured from the center frequency $\omega_0$ of the filter passband given by $\Delta\omega_i = \omega_i - \omega_0$, where $\omega_i$ is the resonant frequency of microring $i$. Denoting $a_i$ as the energy amplitude in microring $i$, the system of $N$ mutually-coupled microring resonators in Fig. 1 can be described by the matrix equation [8]

$$(s\mathbf{I} + \mathbf{L} + j\mathbf{M})\mathbf{a} = \mathbf{b}\,, \tag{1}$$

where $s = j(\omega - \omega_0)$, $\mathbf{I}$ is the $N\times N$ identity matrix, and $\mathbf{a}$ and $\mathbf{b}$ are $N\times 1$ vectors given by

$$\mathbf{a} = [a_1, \quad a_2, \quad a_3, \quad \ldots \quad a_N]^T\,,$$

$$\mathbf{b} = [-j\mu_i s_i, \quad 0, \quad 0, \quad \ldots \quad 0]^T\,.$$

The matrix $\mathbf{M}$ in Eq. (1) represents the coupling topology and has the general symmetric form

#82796 - $15.00 USD Received 7 May 2007; revised 9 Jul 2007; accepted 16 Jul 2007; published 19 Jul 2007

$$\mathbf{M} = \begin{bmatrix} \Delta\omega_1 & \mu_{1,2} & \mu_{1,3} & \cdots & \mu_{1,N} \\ \mu_{1,2} & \Delta\omega_2 & \mu_{2,3} & \cdots & \mu_{2,N} \\ \mu_{1,3} & \mu_{2,3} & \Delta\omega_3 & \cdots & \mu_{3,N} \\ \vdots & \vdots & \vdots & \ddots & \vdots \\ \mu_{1,N} & \mu_{2,N} & \mu_{3,N} & \cdots & \Delta\omega_N \end{bmatrix}, \tag{2}$$

where the diagonal elements of the matrix represent the frequency detunings of the microrings and the off-diagonal elements are the inter-ring coupling coefficients. The matrix **L** is a diagonal matrix which represents the rates of energy lost or extracted from the system. If all the microrings are assumed to be lossless, then **L** is simply an $N \times N$ zero matrix except for the elements $L_{11} = \mu_i^2 / 2$ and $L_{NN} = \mu_o^2 / 2$, which represent the rates of energy coupling to the input and output bus waveguides, respectively. Solution of the matrix equation (1) gives the amplitudes $a_i$ of the energies stored in the microrings, from which the transmitted and reflected spectral responses of the filter can be obtained via

$$\frac{s_t}{s_i} = -\frac{j\mu_o a_N}{s_i}, \tag{3}$$

$$\frac{s_r}{s_i} = 1 - \frac{j\mu_i a_1}{s_i}. \tag{4}$$

Given a symmetric spectral response, a procedure for synthesizing a microring filter having the general coupling topology of Fig. 1 has been discussed in [8]. The transfer function of such a filter is described by a ratio of polynomials with real coefficients. Here we extend the technique to synthesize microring filters with asymmetric spectral characteristics, whose transfer functions are described in general by a ratio of polynomials with complex coefficients,

$$H(s) = \frac{\prod_{k=1}^{N-2}(s - z_k)}{\prod_{k=1}^{N}(s - p_k)} = \frac{\sum_{k=0}^{N-2} b_k s^k}{\sum_{k=0}^{N} a_k s^k} = \frac{P(s)}{Q(s)}. \tag{5}$$

In the above, $z_k$ and $p_k$ denote the zeros and poles, respectively, of the filter which are in general unpaired complex numbers, and $a_k$ and $b_k$ are the complex coefficients of polynomials $Q(s)$ and $P(s)$, which are of degrees $N$ and $N$–2, respectively. The transfer function $H(s)$ in (5) represents the response of the prototype filter with cut-off frequency $\omega_c$ = 1 rad/s. The filter synthesis procedure developed in [8] involves constructing an equivalent electrical circuit model for the system of coupled microring resonators, then applying the well-known coupling-matrix technique for synthesizing microwave filters to realize the desired optical response [14–18]. For optical filters, the coupling-matrix method has been shown to provide reasonably accurate synthesis of filters whose bandwidth is much smaller than the FSR, which is also the condition for the energy coupling model to be valid [8]. In the following we summarize the above filter synthesis procedure as it is applied to asymmetric microring filters.

The equivalent electrical circuit model of the general coupled-microring filter topology in Fig. 1 consists of a network of coupled *LC* resonators which can be described by the same coupling matrix **M** in (2). Since **M** is real and symmetric, it can be factored in the form [8,15]

$$\mathbf{M} = \mathbf{T} \cdot \mathbf{\Lambda} \cdot \mathbf{T}^t, \tag{6}$$

where **T** is a real orthonormal matrix and **Λ** is a diagonal matrix containing the eigenvalues $\lambda_k$ of **M**. The filter synthesis procedure thus involves determining the matrices **Λ** and **T** for a

#82796 - $15.00 USD Received 7 May 2007; revised 9 Jul 2007; accepted 16 Jul 2007; published 19 Jul 2007

given filter transfer function $H(s)$ in (5). In the well-known coupling-matrix technique for synthesizing microwave filters, the elements of $\mathbf{\Lambda}$ and $\mathbf{T}$ can be extracted from the short-circuit admittance parameters $\mathbf{Y}_{sc}$ of the equivalent circuit network, which can be expressed in the form [15]

$$\mathbf{Y}_{sc} = \begin{bmatrix} y_{11} & y_{12} \\ y_{21} & y_{22} \end{bmatrix} = \sum_{k=1}^{N} \frac{1}{s - j\lambda_k} \begin{bmatrix} \xi_{11}^{(k)} & \xi_{12}^{(k)} \\ \xi_{21}^{(k)} & \xi_{22}^{(k)} \end{bmatrix}. \tag{7}$$

In the above, $\xi_{i,j}^{(k)}$ is the residue of admittance $y_{i,j}$ at the pole $\lambda_k$, which is also an eigenvalue of the coupling matrix $\mathbf{M}$. Thus the matrix $\mathbf{\Lambda}$, which is real, can be constructed from the poles $\lambda_k$ of $\mathbf{Y}_{sc}$. Due to the reciprocal nature of the network, we have $y_{12} = y_{21}$ and also $y_{11} = y_{22}$, or equivalently, $\xi_{12}^{(k)} = \xi_{21}^{(k)}$ and $\xi_{11}^{(k)} = \xi_{22}^{(k)}$. The admittance residues $\xi_{11}^{(k)}$ are real while $\xi_{12}^{(k)}$ are imaginary, but unlike the case of symmetric filters, $\xi_{12}^{(k)}$ does not appear in conjugate pairs. From $\xi_{11}^{(k)}$ we can compute the input and output coupling coefficients of the microring filter via

$$\mu_i^2 = \mu_o^2 = 2\sum_{k=1}^{N} \xi_{11}^{(k)} . \tag{8}$$

The elements in the first and last rows of the matrix $\mathbf{T}$ are next determined from

$$T_{1,k} = \frac{\sqrt{2\xi_{11}^{(k)}}}{\mu_i}, \tag{9}$$

$$T_{N,k} = T_{1,k}\,\mathrm{sgn}\left\{\mathrm{imag}\left\{\xi_{12}^{(k)}\right\}\right\}. \tag{10}$$

The remaining rows of $\mathbf{T}$ can be obtained by Gram-Schmidt orthogonalization since the matrix $\mathbf{T}$ is orthonormal. The coupling matrix $\mathbf{M}$ is next determined from $\mathbf{T}$ and $\mathbf{\Lambda}$ using (6). Finally, frequency scaling is applied to the prototype design to obtain the coupling coefficients for the filter with the specified bandwidth $B$ according to $\mu_i \to \mu_i\sqrt{B/2}$, $\mu_o \to \mu_o\sqrt{B/2}$ and $\mu_{i,j} \to \mu_{i,j}(B/2)$.

The short-circuit admittance matrix $\mathbf{Y}_{sc}$ of the equivalent circuit network can be determined if the through-port response of the microring filter is known. Given a specified drop-port filter transfer function $H(s)$ of the form in (5), the through-port response $F(s)$ can be obtained from the factorization,

$$F(s)F(-s) = 1 - H(s)H(-s) . \tag{11}$$

Since the through-port response $F(s)$ is also the reflection coefficient $\Gamma(s)$ of the equivalent electrical circuit, we can obtain an expression for the input impedance $Z_{in}(s)$ of the equivalent circuit from

$$Z_{in}(s) = \frac{1 + F(s)}{1 - F(s)} = \frac{Q(s) + R(s)}{Q(s) - R(s)}, \tag{12}$$

where $R(s)$ is an $N$th-degree polynomial such that $F(s) = R(s)/Q(s)$. From the above expression for $Z_{in}$, the short-circuit admittance parameters $\mathbf{Y}_{sc}$ can be determined using a similar procedure as in [17]. Specifically, if $Z_{in}(s)$ is expressed as

#82796 - $15.00 USD Received 7 May 2007; revised 9 Jul 2007; accepted 16 Jul 2007; published 19 Jul 2007

$$Z_{in}(s) = \frac{m(s) + n(s)}{Q(s) - R(s)}, \tag{13}$$

where $m(s)$ and $n(s)$ are polynomials constructed from the complex coefficients $a_k$ and $c_k$ of $Q(s)$ and $R(s)$, respectively, according to

$$m(s) = \mathrm{Re}\{a_0 + c_0\} + j\,\mathrm{Im}\{a_1 + c_1\}s + \mathrm{Re}\{a_2 + c_2\}s^2 + j\,\mathrm{Im}\{a_3 + c_3\}s^3 + \ldots \tag{14}$$

$$n(s) = j\,\mathrm{Im}\{a_0 + c_0\} + \mathrm{Re}\{a_1 + c_1\}s + j\,\mathrm{Im}\{a_2 + c_2\}s^2 + \mathrm{Re}\{a_3 + c_3\}s^3 + \ldots, \tag{15}$$

then it can be shown that the elements of $\mathbf{Y}_{sc}$ are given by [17]

$$y_{11}(s) = y_{22}(s) = \begin{cases} n(s)/m(s), & \text{if } N \text{ is even,} \\ m(s)/n(s), & \text{if } N \text{ is odd,} \end{cases} \tag{16}$$

$$y_{12}(s) = y_{21}(s) = \begin{cases} P(s)/m(s), & \text{if } N \text{ is even,} \\ P(s)/n(s), & \text{if } N \text{ is odd.} \end{cases} \tag{17}$$

By performing partial fraction expansion of $y_{11}(s)$ and $y_{12}(s)$ in the form of (7), the poles $\lambda_k$ and residues $\xi_{11}^{(k)}$ and $\xi_{12}^{(k)}$ can be obtained, from which the coupling matrix **M** can be determined.

The initial coupling matrix **M** obtained using the above procedure may represent a coupling topology that is not realizable due to physical layout constraints, such as when a microring is required to couple to too many other microrings. Another non-realizable coupling topology, shown in Fig. 2, is the formation of a triplet or more generally, a circular arrangement consisting of an odd number of resonators. These structures lead to coupling between the forward and backward propagating modes in the microrings and results in a reflected wave at the input port. A non-realizable coupling topology may be converted into a realizable configuration by performing similarity transformations such as Jacobi rotation and reflection on the original matrix **M** to obtain a new coupling matrix **M′** given by [15,17]

$$\mathbf{M}' = \mathbf{R}(\theta_r) \cdot \mathbf{M} \cdot \mathbf{R}^t(\theta_r). \tag{18}$$

In the above $\mathbf{R}(\theta_r)$ is an $N \times N$ rotation matrix and $\theta_r$ is the rotation angle chosen to annihilate unrealizable coupling elements in the original coupling matrix **M**. In addition, we can also use similarity transformations to generate alternative coupling configurations with different sets of coupling coefficients and microring detunings. Out of these possible filter designs, an optimum device topology may then be chosen which has the minimum number of coupling elements as well as coupling values that are more easily realized. For example, it is generally desirable to minimize the number of negative coupling elements in the device since they require long optical coupling lengths (between $3\pi/2$ and $2\pi$) or precise layout geometry [10] and are thus more difficult to realize than positive couplings.

#82796 - $15.00 USD Received 7 May 2007; revised 9 Jul 2007; accepted 16 Jul 2007; published 19 Jul 2007

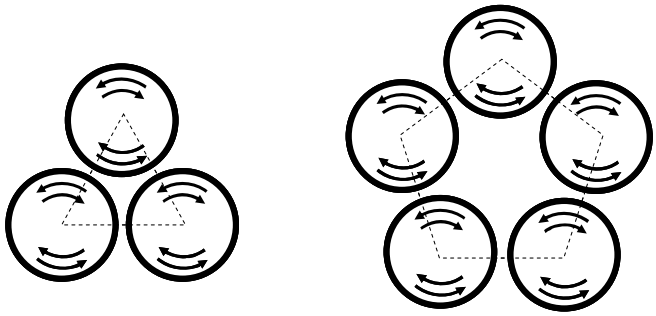

(a) (b)

Fig. 2. Examples of filter coupling topologies that are not realizable with microring resonators: (a) a triplet; (b) a quintuplet. In general a circular arrangement consisting of an odd number of microrings will lead to coupling between counter-propagating modes.

For asymmetrical filters the diagonal elements of the coupling matrix **M** are in general non-zero, indicating that the microrings will have some detunings with respect to the center filter frequency. These detunings are usually small and do not give rise to the Vernier effect, so that the transmission bands at adjacent FSRs are not suppressed. On the other hand, symmetric filters may be realized using either synchronous or asynchronous microrings. By allowing the resonators to take on detuning values, alternative asynchronous designs can be obtained which may be easier to implement than their synchronous counterparts. In this respect, asynchronicity provides an added degree of flexibility in the design of coupled-microring filters. Also, different filter topologies in general have different sensitivity performance with respect to variations in the coupling parameters. A simple tolerance analysis of coupled-microring filters with symmetric spectral responses has been given in [8], and a similar procedure may be applied to asymmetric microring filters. By performing tolerance analysis of the filter response subject to random parameter variations for each of the alternative filter designs, a robust device architecture may be chosen which exhibits the highest tolerance to fabrication errors.

## 3. Numerical examples of asymmetric optical filters

We illustrate the above synthesis procedure with two asymmetric filter designs, one being an odd-order filter and the other an even-order filter. The first example is a 7-pole filter with 2 transmission zeros on the right or high-frequency side of the passband, and 1 transmission zero on the left or low-frequency side. This example illustrates how the transmission zeros of a filter can be freely moved in order to achieve a different roll-off rate and out-of-band rejection level on each side of the transmission band. The second design is a 6-pole filter with two transmission zeros both moved to the right-hand side of the passband and no zeros on the left-hand side. This example shows that for a given number of transmission zeros, the sharpest transition can be achieved on one side of the passband by moving all the zeros to that side.

### *3.1. Seventh-order microring filter with 3 transmission zeros*

We consider the design of an asymmetric $7^{th}$-order microring filter with a 25GHz bandwidth. On the right-hand side of the passband, two transmission zeros are placed close to the band edge to achieve a very steep roll-off and an out-of-band rejection level of –55dB. On the left-hand side, the roll-off requirement is more relaxed so only one zero is needed, but the out-of-band rejection should be –65dB. The locations of the poles and zeros required to realize the filter transfer function are listed in Table 1. Also shown in the table are the poles of the short-circuit admittances, $y_{11}$ and $y_{12}$, as well as their residues, $\xi_{11}$ and $\xi_{12}$, which were obtained

#82796 - $15.00 USD Received 7 May 2007; revised 9 Jul 2007; accepted 16 Jul 2007; published 19 Jul 2007

from the transfer function. In the filter synthesis procedure, the input and output energy coupling coefficients of the microring filter were first computed using Eq. (8) to give $\mu_i = \mu_o = 1.2843$, or 11.3816 after bandwidth scaling. The coupling matrix of the filter was obtained next using the procedure described in the previous section, yielding

$$\mathbf{M} = \begin{bmatrix} 0.8923 & -22.3716 & -22.8255 & 35.1739 & -29.4535 & -20.9037 & 0 \\ & -67.7296 & 6.7356 & 7.3705 & 18.8095 & -20.2062 & -14.0854 \\ & & -55.0406 & -11.8001 & 1.1817 & -27.2934 & 35.2899 \\ & & & 34.8664 & -4.2710 & -13.7113 & -25.1258 \\ & & & & -28.3751 & -3.1199 & -27.3435 \\ & & & & & 61.4286 & -27.2107 \\ & & & & & & 0.8923 \end{bmatrix}, \quad (19)$$

Table 1. Columns 1 and 2: poles and zeros of the transfer function of the 7th-order asymmetric filter; Columns 3–5: poles and residues of the short-circuit admittance parameters of the equivalent electrical network.

| Filter poles, $p_k$ | Filter zeros, $z_k$ | Poles of $y_{11}$ and $y_{12}$ | $\xi_{11}$ | $\xi_{12}$ |
|---|---|---|---|---|
| $-0.0956 - j1.0472$ | $-j2.000$ | $-j1.1206$ | 0.0695 | $j0.0695$ |
| $-0.2825 - j0.8047$ | $j1.2153$ | $j1.0716$ | 0.0473 | $j0.0473$ |
| $-0.4121 - j0.3358$ | $j1.4030$ | $j1.0279$ | 0.0911 | $-j0.0911$ |
| $-0.0363 + j1.0201$ | | $-j0.9279$ | 0.1522 | $-j0.1522$ |
| $-0.1343 + j0.9311$ | | $j0.7625$ | 0.1199 | $j0.1199$ |
| $-0.2807 + j0.6843$ | | $-j0.3922$ | 0.1757 | $j0.1757$ |
| $-0.4079 + j0.2278$ | | $j0.2543$ | 0.1690 | $-j0.1690$ |

where only the upper half of the coupling matrix is shown since **M** is symmetric. The coupling topology described by the matrix **M** above is not physically realizable with microring resonators since the matrix is almost full, requiring every microring to couple to every other microring except between resonators 1 and 7. To convert the above coupling topology into one which is physically realizable and much more simplified, we performed a series of rotations on the original matrix **M** following a procedure described in [18] to annihilate the unrealizable coupling elements as well as minimize the number of couplings. The new matrix obtained, which contains only 7 coupling elements, is given by

$$\mathbf{M}' = \begin{bmatrix} 0.8923 & 42.2088 & 0 & 0 & 0 & 42.2088 & 0 \\ & 4.7966 & 44.4642 & 0 & 0 & 0 & 42.2088 \\ & & -33.5104 & 0 & 0 & 0 & 0 \\ & & & -58.6984 & 41.5723 & 0 & 0 \\ & & & & 35.3269 & 45.1662 & 0 \\ & & & & & -2.7650 & -42.2088 \\ & & & & & & 0.8923 \end{bmatrix}. \quad (20)$$

#82796 - $15.00 USD Received 7 May 2007; revised 9 Jul 2007; accepted 16 Jul 2007; published 19 Jul 2007

The coupling topology corresponding to the new matrix is shown in Fig. 3. As indicated in the figure, each microring in the filter supports only one unidirectionally-propagating mode and coupling between counter-propagating waves does not arise. We also note that the nonzero diagonal elements in the coupling matrix indicate the amount of detuning ($\Delta\omega$, $\times 10^9$ rad/s) from the center frequency $\omega_0$ of each microring in the filter. In practice these small detunings may be realized by thermal-optic or electro-optic control of the index of the microring waveguides.

The coupling matrix in Eq. (20) contains only one negative coupling element, namely the term $\mu_{6,7}$. It is well-known that coupled-cavity filters with transmission zeros require non-adjacent cavity coupling with at least one negative coupling element, such as the quadruplet coupling configuration formed by microrings 1-2-7-6 in Fig. 3. The filter topology in Fig. 3, which is known as the "cul-de-sac" configuration in microwave filters, has the important advantage that there is only one negative coupling element in the entire network as long as the number of transmission zeros is less than $N$–2 [12,18]. In optical microring filters, negative couplings may be achieved by evanescent coupling between the straight waveguide sections of adjacent microracetrack resonators, with the coupling length $L$ satisfying $3\pi/2 < k_c L < 2\pi$, where $k_c$ is the per-unit-length coupling strength. Alternatively, it was recently suggested that negative coupling may also be achieved by a $\lambda/8$ shearing rotation of the coupling axis of the quadruplet [10]. It should also be noted that for microring resonators arranged in a loop-coupling configuration, such as the quadruplet in Fig. 3, the positions of the coupling points between adjacent microrings do affect the coupling signs so that care must be exercised in laying out the device geometry. By contrast, there is no restriction on the positions of the coupling points for microrings 3, 4 and 5.

In Fig. 4 we plotted the spectral responses at the drop port and through port of the synthesized filter, along with the target transfer functions $H(s)$ and $F(s)$. It is seen that the synthesized responses agree very well with the specified filter characteristics. The placement of two transmission zeros on the right-hand side of the passband results in a much steeper roll-off on that side compared to the left-hand side. By varying the positions of the zeros, a trade-off between the roll-off rate and out-of-band rejection level can be obtained to suit a specific application. For comparison we also plotted the transmission response of a 7$^{th}$-order Butterworth filter having the same bandwidth of 25GHz. The superior performance of the asymmetric filter is apparent from the much sharper band transitions and higher isolation levels compared to the Butterworth filter. In Fig. 5 we plotted the group delay response of the filter, which also exhibits an asymmetric spectral shape. Specifically, the group delay is seen to be higher near the right band edge, which corresponds to the steeper amplitude transition compared to the left-hand side.

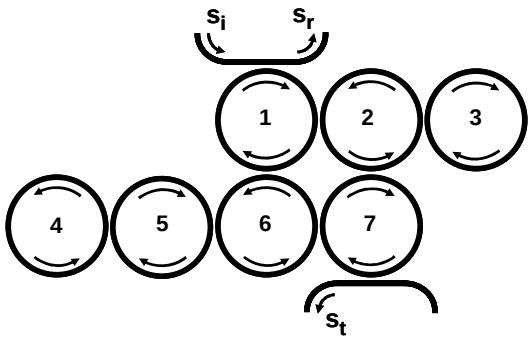


Fig. 3. Optimum coupling topology of a 7-pole, 3-zero asymmetric microring filter.

#82796 - $15.00 USD Received 7 May 2007; revised 9 Jul 2007; accepted 16 Jul 2007; published 19 Jul 2007

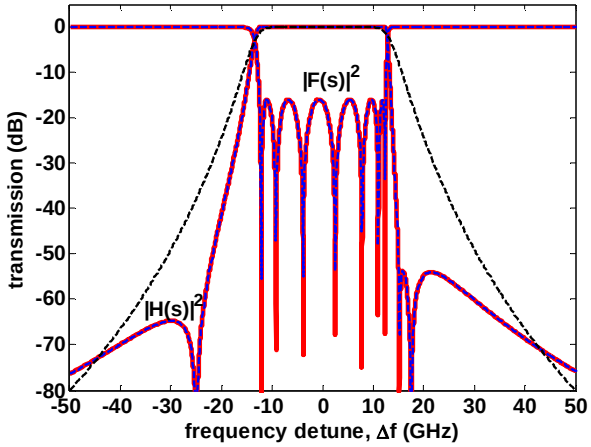


Fig. 4. Spectral responses at the drop port, $|H(s)|^2$, and through port, $|F(s)|^2$, of the 7-pole, 3-zero, 25GHz asymmetric microring filter. Solid red lines are the responses of the synthesized filter; dashed blue lines are the target responses; dashed black line represents the response of a 7th-order, 25GHz Butterworth filter.

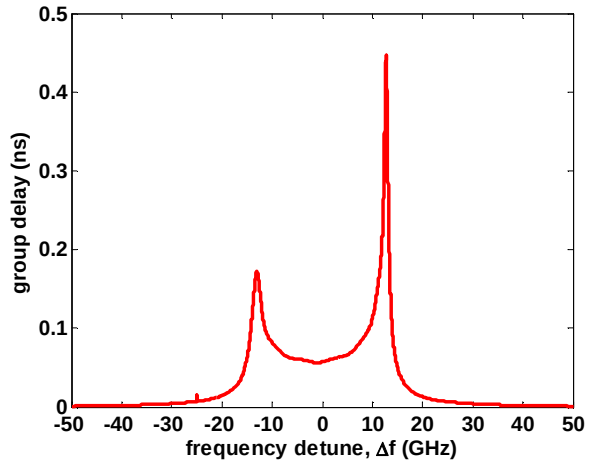


Fig. 5. Group delay response of the 7th-order, 25GHz asymmetric microring filter.

### *3.2. Sixth-order microring filter with 2 transmission zeros*

In this example we consider the design of an asymmetric 6th-order, 10GHz-bandwidth filter with two transmission zeros. The requirement here is to maximize the roll-off rate on the high-frequency side of the passband while maintaining a –45dB out-of-band rejection level. If there is no additional constraint specified for the low-frequency side of the passband, we can move both transmission zeros of the filter to the right-hand side. The poles and zeros of the filter transfer function which satisfies the above requirements are given in columns 1 and 2 of Table 2. The corresponding poles and residues of the short-circuit admittance parameters of the equivalent circuit are also shown in the table. Application of the filter synthesis procedure in Section 2 yielded the input and output coupling coefficients $\mu_i = \mu_o = 6.8971$ and optimized coupling matrix $\mathbf{M}'$ given by

#82796 - $15.00 USD Received 7 May 2007; revised 9 Jul 2007; accepted 16 Jul 2007; published 19 Jul 2007

$$\mathbf{M}' = \begin{bmatrix} 0.8391 & 16.5149 & 0 & 0 & 16.5149 & 0 \\ & 7.0767 & 23.4082 & 0 & 0 & 16.5149 \\ & & -6.5692 & 0 & 0 & 0 \\ & & & -29.5817 & 6.5533 & 0 \\ & & & & -4.9346 & -16.5149 \\ & & & & & 0.8391 \end{bmatrix}. \quad (21)$$

The device topology associated with the above coupling matrix is shown in Fig. 6. We plotted the drop-port and through-port responses of the synthesized filter in Fig. 7(a), where it can be seen that the filter exhibits a much steeper roll-off on the right-hand side of the passband than on the left side. The sharp transition between the passband and stopband at the high-frequency side is shown in more detail in Fig. 7(b). The abrupt band transition coupled with a very high out-of-band rejection level makes this type of asymmetric filters suitable for applications where a high level of frequency discrimination is required, such as in the separation of two closely-spaced optical signals. In Fig. 8 we plotted the group delay response of the filter (solid red line), which is seen to exhibit much stronger phase dispersion near the right band edge than the left side as expected.

Table 2. Columns 1 and 2: poles and zeros of the transfer function of the 6th-order asymmetric filter; Columns 3–5: poles and residues of the short-circuit admittance parameters of the equivalent electrical network.

| Filter poles, $p_k$ | Filter zeros, $z_k$ | Poles of $y_{11}$ and $y_{12}$ | $\xi_{11}$ | $\xi_{12}$ |
|---|---|---|---|---|
| $-0.1715 - j1.0598$ | $j1.1530$ | $-j1.1361$ | 0.0968 | $-j0.0968$ |
| $-0.4216 - j0.5922$ | $j1.3360$ | $j1.0543$ | 0.0366 | $j0.0366$ |
| $-0.4554 + j0.0894$ | | $j1.0063$ | 0.0820 | $-j0.0820$ |
| $-0.3037 + j0.6494$ | | $j0.7133$ | 0.1343 | $j0.1343$ |
| $-0.1302 + j0.9275$ | | $-j0.6957$ | 0.2077 | $j0.2077$ |
| $-0.0318 + j1.0148$ | | $j0.0870$ | 0.1998 | $-j0.1988$ |

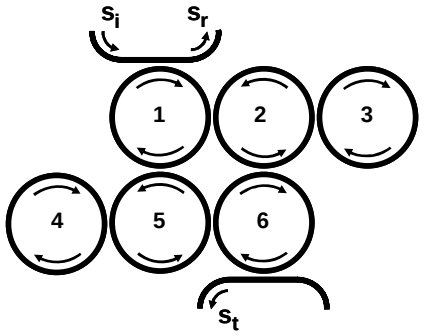


Fig. 6. Optimum coupling topology of a 6-pole, 2-zero asymmetric microring filter.

#82796 - $15.00 USD Received 7 May 2007; revised 9 Jul 2007; accepted 16 Jul 2007; published 19 Jul 2007

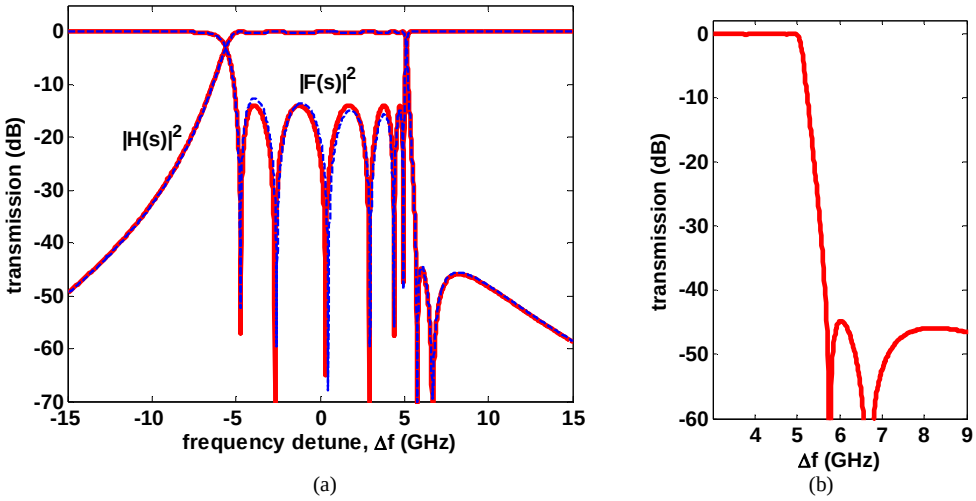


(a) (b)

Fig. 7. (a) Spectral responses at the drop port, $|H(s)|^2$, and through port, $|F(s)|^2$, of the 6-pole, 2-zero asymmetric microring filter. Solid red lines are the responses of the synthesized filter; dashed blue lines are the exact filter responses obtained from power coupling analysis. (b) Transition at the right band edge of the drop-port response of the filter.

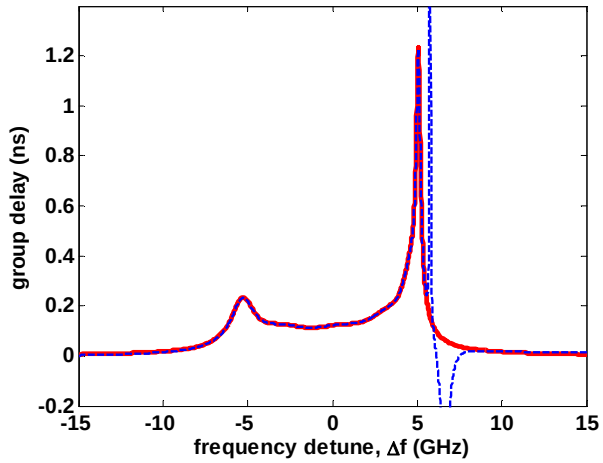


Fig. 8. Group delay response of the 6th-order, 10GHz asymmetric microring filter. Solid red line is the response of the synthesized filter; dashed blue line is the exact response obtained from power coupling analysis.

#82796 - $15.00 USD Received 7 May 2007; revised 9 Jul 2007; accepted 16 Jul 2007; published 19 Jul 2007

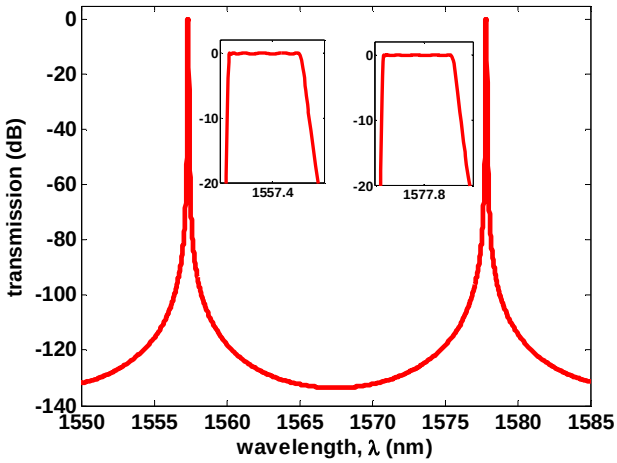


Fig. 9. Broadband characteristic across one free spectral range of the 6th-order asymmetric microring filter. The insets give the closed-up views of the passbands at λ = 1557.4nm and λ = 1577.8nm.

The filter design given by the coupling matrix **M** in Eq. (21) was obtained using the approximate energy coupling formalism. To verify the validity of the energy model used, we also performed analysis of the synthesized microring filter using the power coupling method, which allows the exact device spectral responses to be determined. In the power analysis we assumed the microring resonators to have a nominal free spectral range of 2.5THz (20nm), which may be realized using a high-index material system such as Silicon-on-Insulator or III-V semiconductor compounds. Also, the filter passband was assumed to be centered at the 1.557μm wavelength. The exact amplitude responses at the drop port and through port, and the group delay of the filter obtained from the power analysis are shown by the blue dashed lines in Fig. 7(a) and Fig. 8. The results are seen to agree very well with the responses of the synthesized filter obtained using the energy-coupling approximation. For the group delay in Fig. 8, the spikes in the response obtained from the power analysis occur at the transmission zeros where the phase is not well defined. These frequencies also lie outside the passband and are thus usually of little interest. The power coupling method also allows us to investigate the broadband response of the filter over more than one free spectral range. In Fig. 9 we plotted the transmission characteristic of the filter at the drop port as a function of the wavelength across one FSR. It is seen that even though all the microrings in the filter design are detuned from each other, virtually no Vernier effect is observed since adjacent passbands are not suppressed or distorted, as shown by the insets of the figure, and the FSR of the filter is the same as that of the individual microrings.

## 4. Conclusion

We proposed and demonstrated the use of asynchronously-tuned, coupled-microring resonators for realizing high-order optical filters with asymmetric spectral responses. These devices offer more design flexibility than conventional symmetric filters in achieving an optimum spectral response that best suits the demands or technological constraints of a specific application. Moreover, by allowing the microrings to be slightly detuned from each other, alternative filter topologies can be obtained that may be easier to implement or more tolerant to fabrication errors than designs using only synchronous resonators. A method for synthesizing a given filter transfer function based on the energy coupling matrix was also presented along with numerical examples of high-order asymmetric microring filters. The

#82796 - $15.00 USD Received 7 May 2007; revised 9 Jul 2007; accepted 16 Jul 2007; published 19 Jul 2007

proposed filter topology and synthesis method can also be applied to photonic crystal nanocavities to realize extremely compact devices. These coupled-microring and coupled-nanocavity filters enable a considerably wider range of optical spectral responses to be realized than currently possible, and are thus expected to have important applications in amplitude and phase filtering, optical spectral shaping and dispersion engineering.

#82796 - $15.00 USD Received 7 May 2007; revised 9 Jul 2007; accepted 16 Jul 2007; published 19 Jul 2007